

Optical study of superconducting Ga-rich layers in silicon

T. Fischer,* A. V. Pronin,[†] R. Skrotzki, T. Herrmannsdörfer, and J. Wosnitza
*Dresden High Magnetic Field Laboratory (HLD),
Helmholtz-Zentrum Dresden-Rossendorf, 01314 Dresden, Germany*

J. Fiedler, V. Heera, and M. Helm
*Institute of Ion Beam Physics and Materials Research,
Helmholtz-Zentrum Dresden-Rossendorf, 01314 Dresden, Germany*

E. Schachinger
*Institute of Theoretical and Computational Physics,
Graz University of Technology, 8010 Graz, Austria*

(Dated: November 1, 2018)

We performed phase-sensitive terahertz (0.12 – 1.2 THz) transmission measurements of Ga-enriched layers in silicon. Below the superconducting transition, $T_c^{\text{middle}} = 6.7$ K, we find clear signatures of the formation of a superconducting condensate and of the opening of an energy gap in the optical spectra. The London penetration depth, $\lambda(T)$, and the condensate density, $n_s = \lambda^2(0)/\lambda^2(T)$, as functions of temperature demonstrate behavior, typical for conventional superconductors with $\lambda(0) = 1.8 \mu\text{m}$. The terahertz spectra can be well described within the framework of Eliashberg theory with strong electron-phonon coupling: the zero-temperature energy gap is $2\Delta(0) = 2.64$ meV and $2\Delta(0)/k_B T_c = 4.6 \pm 0.1$, consistent with the amorphous state of Ga. At temperatures just above T_c , the optical spectra demonstrate Drude behavior.

PACS numbers: 74.25.Gz, 74.70.Ad, 74.78.-w, 74.25.nd

I. INTRODUCTION

Recently, some of us observed superconductivity in amorphous Ga-rich layers manufactured by Ga implantation into Si wafers and subsequent thermal annealing.¹ Compared to bulk crystalline Ga, superconductivity occurs at higher temperatures with an onset at 7 – 10 K. While previously, amorphous Ga films have only been characterized subsequently to *in situ* low-temperature synthesis,^{2,3} the films under investigation withstand multiple cooling procedures and room-temperature handling.

Here, we report optical evidence for the superconducting-state formation in gallium-enriched layers in silicon by means of optical measurements in the terahertz region. These layers consist of amorphous, gallium-rich precipitates embedded in nanocrystalline silicon.⁴ Optical spectra of superconductors contain valuable information about the superconducting state: the London penetration depth, the strength of coupling, the size and the symmetry of the superconducting gap can be extracted from such measurements.^{5,6}

In our optical measurements within the terahertz region, we observe clear signatures of the superconducting condensate developing at $T < T_c$. We were able to trace the temperature dependence of the spectral weight of the condensate and of the London penetration depth. We demonstrate that they follow nicely the behavior expected for fully gaped superconductors. We further show that the frequency-dependent optical spectra can be well described within the Eliashberg theory for strong-coupling *s*-wave superconductors.

II. EXPERIMENT

Ga⁺ ions had been implanted at an energy of 80 keV with a total fluence of $4 \times 10^{16} \text{ cm}^{-2}$ Ga into 0.38 mm thick (100)-oriented silicon wafers covered with 30 nm of silicon dioxide. Subsequent rapid thermal annealing at 650 °C for 60 seconds has been applied for realizing gallium precipitation at the Si – SiO₂ interface. The thickness of the fabricated Ga-rich layers was estimated to be 10 nm by means of transmission electron microscopy and Rutherford backscattering.⁴ The samples probed optically had lateral sizes of 2 by 5 mm. Direct-current resistivity measurements (Fig. 1) show the onset of the superconducting transition at $T_c^{\text{onset}} \approx 7.3$ K and a middle point at $T_c^{\text{middle}} = 6.7$ K, which we take as T_c for our Eliashberg analysis below. Further information, such as a detailed structural and critical-field analysis, can be found in Refs. 1 and 4.

In the frequency range 3.9 - 41 cm⁻¹ (117 - 1230 GHz, 0.48 - 5.1 meV), measurements have been performed by use of a spectrometer, equipped with backward-wave oscillators (BWOs) as sources of coherent and frequency-tunable radiation. The measurements have been done using a number of different BWOs covering the above-mentioned frequency range almost continuously.

A Mach-Zehnder interferometer arrangement of the spectrometer allows to measure both the intensity and the phase shift of the wave transmitted through the sample. A commercial optical ⁴He cryostat with the sample inside is installed in one of the arms of the interferometer. A mirror in another (reference) arm is connected to a precision stepper motor (with an accuracy of 0.5 μm).

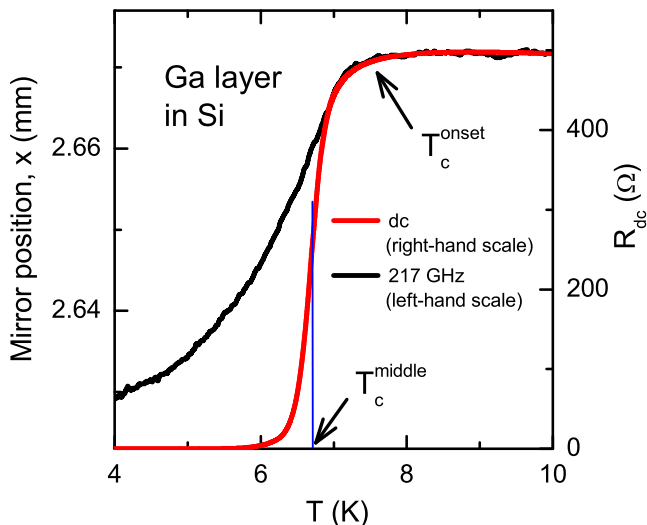


FIG. 1: (Color online) Temperature dependence of the resistance of a Ga-enriched layer in Si (right-hand scale) and an example of the raw measurements of the interferometer mirror position (left-hand scale). The mirror position is directly related to the optical phase shift and, hence, to the permittivity and the penetration depth.

The interferometer can be adjusted to a position, where the optical path difference between the arms is zero. During frequency or temperature sweeps, a software always keeps the movable mirror in position with zero optical path difference. Any change in the sample's refraction index (or dielectric permittivity) results in a change of the optical path length in the sample arm, and, hence, to a shift of the movable mirror. This shift is detected and the phase change of the wave transmitted through the sample is directly calculated from it. For the amplitude transmission measurements, the reference arm of the interferometer is blocked with a shutter. The absolute values of the sample's amplitude and phase-shift transmission, Tr and φ , are obtained by repeating the measurements without a sample and a subsequent correction for the empty-channel measurement. Fresnel optical formulas⁷ are used to extract the optical parameters of the sample (for example, the complex conductivity, $\sigma = \sigma_1 + i\sigma_2$, or the complex permittivity $\varepsilon = \varepsilon' + i\varepsilon''$) from Tr and φ . A detailed description of the measurement technique can be found in Ref. 8. The method has been previously applied to a large number of different superconductors.⁹

The London penetration depth, $\lambda = c/(4\pi\sigma_2\omega)^{1/2}$ (ω is the angular frequency, c is the speed of light), has been determined as a function of temperature at a number of fixed frequencies (123, 172, 217, and 252 GHz, or 4.1, 5.74, 7.24, and 8.4 cm^{-1}) in the same way as described in Refs. 10 and 11. For these measurements, we limited ourselves to our lowest frequencies, as at higher frequencies the contribution of normal electrons to σ_2 becomes significant, thus, a correct determination of λ is difficult.

The optical parameters of pristine wafers had been

measured in advance using the same setup. At $T \leq 15$ K, we found the real part of the dielectric permittivity of the wafers to be independent of temperature and frequency (within our accuracy) and equal to $\varepsilon' = 11.50 \pm 0.05$. An absorption in the wafers was not detectable at these temperatures.

III. RESULTS AND DISCUSSION

A. Temperature sweeps. Temperature dependence of penetration depth and condensate density

Firstly, let us note that the appearance of superconductivity in our sample is confirmed by the raw optical data. In Fig. 1, we show an example of such raw data – the position of the movable mirror of the Mach-Zehnder interferometer, $x(T)$, as a function of temperature. Above the superconducting transition, $x(T)$ is flat. As the sample enters into the superconducting state, $x(T)$ starts to decrease rapidly. This is due to the condensation of electrons. The condensed electrons are represented by a delta function in the real part of the complex conductivity, σ_1 . This delta function leads (*via* the Kramers-Kronig relations) to a divergence in σ_2 (and in ε') at $\omega \rightarrow 0$: $\sigma_2 = ne^2/m\omega$, $\varepsilon' \equiv 1 - 4\pi\sigma_2/\omega = 1 - 4\pi ne^2/m\omega^2$ (n is the charge-carrier concentration, e is the elementary charge, and m is the effective mass of the carriers). One can easily estimate that for conventional superconductors at temperatures well below T_c , the permittivity at (sub)terahertz frequencies is of the order of -10^3 to -10^6 .

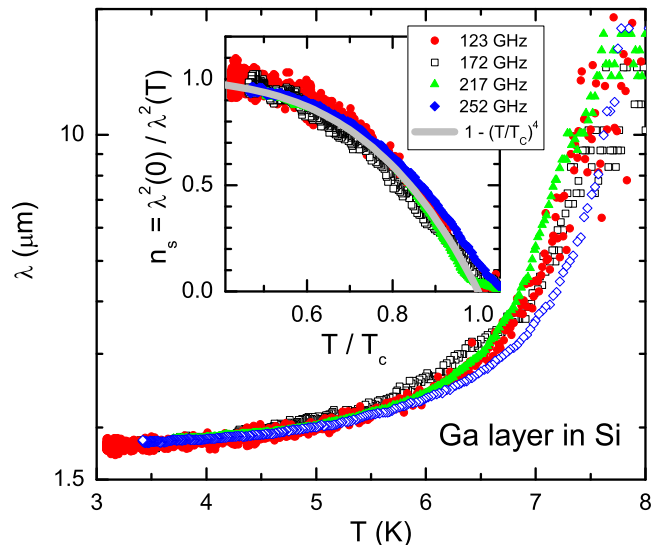


FIG. 2: (Color online) London penetration depth as a function of temperature for some frequencies. Inset: Relative density of superconducting condensate, $n_s = \lambda^2(0)/\lambda^2(T)$, as a function of temperature for the same frequencies as in the main panel. Solid line mimics the behavior expected for a fully gapped superconductor.

This negative ε' leads to a negative contribution to the phase shift and hence to a negative contribution to $x(T)$, directly recorded in our measurements. Obviously, this huge negative ε' is nothing but screening of the probing electromagnetic field by supercurrents. As electrons start to condense already at T_c^{onset} , $x(T)$ begins to decrease starting at this temperature.

The measured temperature dependences of λ for the above-mentioned frequencies are shown in Fig. 2. All curves demonstrate a very similar behavior. At low temperatures, the curves flatten. Extrapolation of $\lambda(T)$ to zero temperature gives $\lambda(0) = (1.8 \pm 0.2) \mu\text{m}$. As the temperature approaches T_c , $\lambda(T)$ nearly diverges for all four frequencies (because at any non-zero frequency, σ_2 is different from zero above T_c , true divergence is not expected).

The inset of Fig. 2 shows the relative density of the superconducting condensate, $n_s = \lambda^2(0)/\lambda^2(T)$, as a function of temperature. All measurements basically fall onto one curve, which can be well approximated by a standard phenomenological expression used to fit the penetration depth data of conventional (fully gapped) superconductors:⁵ $n_s = 1 - (T/T_c)^4$. The highest-frequency curve deviates slightly from the common trend as $T \rightarrow T_c$. We attribute this deviation to the contribution of normal-state carriers, as mentioned above (a similar behavior was observed *e.g.* in Ref. 10). Our measurements are more noisy at lower frequencies because the wavelength of the probing radiation at lower frequencies (123 and 172 GHz) becomes comparable to the lateral sample dimensions.

B. Frequency sweeps. Drude metal and strong-coupling *s*-wave superconductor

Normal state. Figure 3 shows (a) the as-measured transmission, $\text{Tr}(\nu)$, and (b) the phase-shift, $\varphi(\nu)$, spectra as a function of frequency, $\nu = \omega/2\pi$ at 10 K. Since the major term of the phase shift is proportional to the frequency of the probing radiation, the phase-shift spectra are divided by frequency to eliminate the constant frequency slope. The pronounced fringes in both $\text{Tr}(\nu)$ and $\varphi(\nu)$ are due to the multiple interference within the Si substrate, which acts as a Fabry-Perot interferometer.

The spectra can be well fitted by the Drude model, $\sigma(\omega) = \sigma_0/(1 - i\omega\tau)$, where σ_0 is the zero-frequency limit of the conductivity and τ is the scattering time. We find $\sigma_0 = (900 \pm 150) \Omega^{-1}\text{cm}^{-1}$ in good agreement with our dc data [$\sigma_{dc}(10\text{K}) = 1000 \Omega^{-1}\text{cm}^{-1}$]. The scattering rate, $\gamma = 1/(2\pi\tau)$, is above our frequency range. We can estimate, $\gamma \geq 100 \text{ cm}^{-1}$ ($\tau \leq 5.3 \times 10^{-14} \text{ s}$). Lower values of γ would result in an upturn in $\text{Tr}(\nu)$ at the high-frequency end of our range, which we do not observe here. By use of the Fermi velocity for gallium, $v_F = 6 \times 10^7 \text{ cm/s}$,¹² we can estimate the upper limit of the mean free path at 10 K, $\ell \leq 30 \text{ nm}$.

At our high frequencies, we do not see a downturn

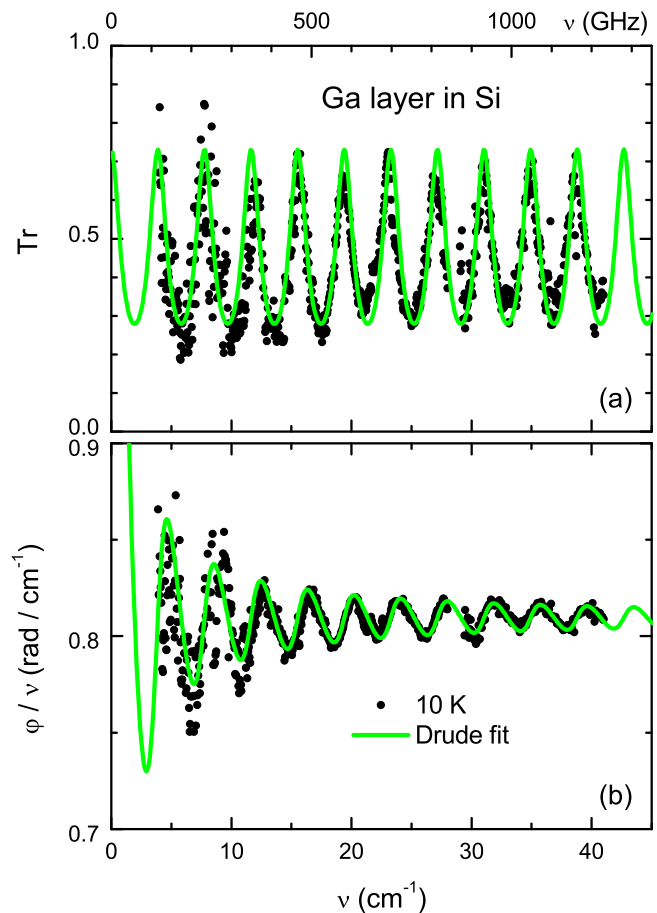


FIG. 3: (Color online) Frequency-dependent amplitude-transmission (a) and phase-shift (b) spectra of the Ga-rich layer in Si at $T = 10 \text{ K}$. Solid lines show a Drude fit. The phase-shift spectra are divided by frequency for better representation.

of transmission either. Such a downturn would indicate greater σ_1 values at higher frequencies and, hence, signal spatial localization of the carriers. Instead, our Drude-type conductivity proves a free-electron transport in the Ga layer. From the value of our highest measurement frequency, we can roughly estimate that no localization happens on scales of a few dozens of nanometers or larger. One cannot, of course, exclude localization effects on smaller spatial scales.

Superconducting state. The changes in the spectra related to superconductivity can best be seen in comparison with the normal-state spectra. Therefore, in Fig. 4, the ratio between the transmission coefficients at 4 and 10 K, Tr_S/Tr_N , is shown in panel (a); the difference between the phase shifts, $\varphi_S - \varphi_N$, measured at the same temperatures, is in panel (b). The presence of fringes in both panels indicates a large change of the dielectric constant, which occurs when the sample enters the superconducting state.

In an attempt to compare experiment with theory we

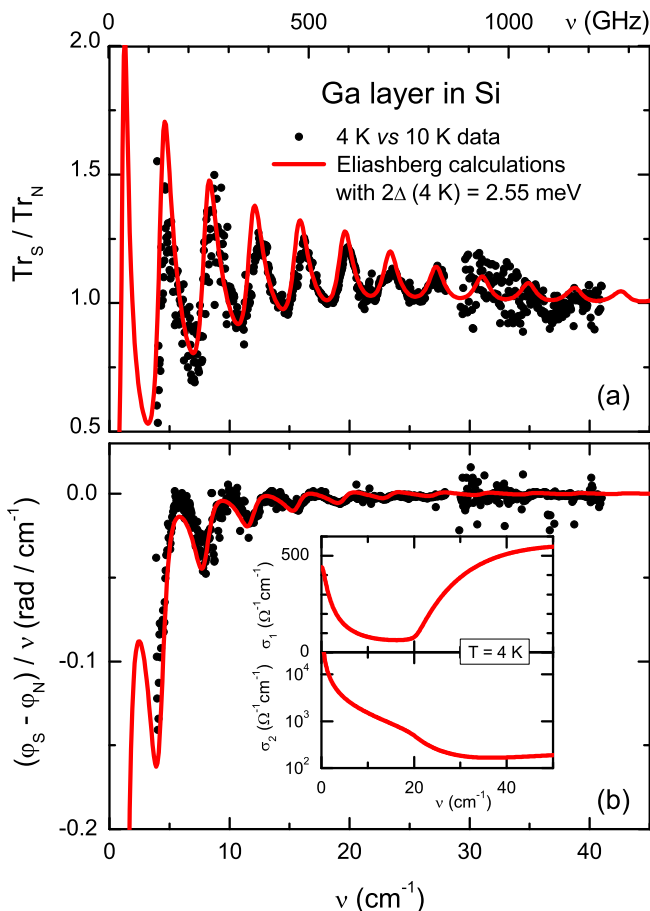


FIG. 4: (Color online) Transmission ratio, Tr_S/Tr_N , (a) and relative phase shift, $\varphi_S - \varphi_N$, (b) for the Ga-rich layer in Si as functions of frequency. Normal-state data are from Fig. 3. Superconducting-state data are collected at 4 K. Solid lines show the Eliashberg calculations for $T = 4\text{ K}$ with $2\Delta(4\text{ K}) = 2.55\text{ meV} = 20.6\text{ cm}^{-1}$. The phase-shift spectra are divided by frequency. The real, $\sigma_1(\nu)$, and imaginary, $\sigma_2(\nu)$, parts of the complex conductivity obtained from the calculations are shown in the insets.

calculated the complex conductivity within the framework of standard s -wave Eliashberg theory.^{13,14} Details of the procedure applied in these calculations will be discussed elsewhere.¹⁵ In agreement with our data on the temperature dependence of the penetration depth and with the amorphous state of Ga in our samples,⁴ we assumed an isotropic s -wave gap. The Eliashberg function, $\alpha^2(\omega)F(\omega)$, and the Coulomb pseudopotential, $\mu^* = 0.17$ have been taken from Ref. 16. The Eliashberg function

was rescaled to give T_c^{middle} keeping μ^* unchanged. This results in a mass-enhancement factor due to electron-phonon interaction of $\lambda_{el-ph} = 1.97$ down from 2.3 as was reported by Chen *et al.*¹⁶ We obtained the zero-temperature energy gap: $2\Delta(0) = 2.64\text{ meV} = 21.3\text{ cm}^{-1}$, and $2\Delta(0)/k_B T_c = 4.6 \pm 0.1$ (the error is estimated from the width of the superconducting transition). This value of $2\Delta(0)/k_B T_c$ is in good agreement with the results of earlier tunneling and infrared experiments on amorphous Ga.^{17–20}

The calculated complex conductivity at $T = 4\text{ K}$ is shown in the insets of Fig. 4 (b). The theoretical complex conductivity is then used to calculate the transmission ratios and the phase-shift difference *via* Fresnel formulas [lines in Fig. 4]. The good agreement between theory and experiment is evident.

Finally, from the obtained value for $2\Delta(0)$, we can estimate the zero-temperature coherence length: $\xi_0 = \hbar v_F / \pi \Delta(0) \cong 100\text{ nm}$. Let us note that although the Ginzburg-Landau coherence length ξ^* derived from the analysis of the upper-critical-field data, was found to be around 10 nm ,¹ there is no contradiction with our result, because ξ^* , derived in that way, is strongly affected by the mean free path.

IV. CONCLUSIONS

Our optical data collected at terahertz frequencies on Ga-enriched layers in Si: i) support the original observation of a superconducting transition in resistivity data¹ *via* the direct detection of the electromagnetic-field screening due to supercurrents; ii) show that the London penetration depth [$\lambda(0) = 1.8\text{ }\mu\text{m}$] and the superconducting condensate density as functions of temperature follow the typical temperature dependence expected for conventional superconductors; iii) prove that the frequency-dependent normal-state conductivity is of Drude type (free electrons) with no signs of localization effects on length scales equal or larger than several dozens of nanometers; iv) indicate that the upper limit of the mean free path ℓ in our sample is roughly 30 nm ; v) allow to estimate the size of the superconducting energy gap, $2\Delta(0) = 2.64\text{ meV}$, and the coherence length, $\xi_0 = 100\text{ nm}$, and to conclude that our sample is a dirty ($\xi_0 > \ell$) strong-coupling ($\lambda_{el-ph} = 1.97$) s -wave superconductor with $2\Delta(0)/k_B T_c = 4.6 \pm 0.1$.

Part of this work was supported by EuroMagNET II (contract 228043) and by the DFG (contract HE 2604/7-1).

* Electronic address: t.fischer@hzdr.de

† Electronic address: a.pronin@hzdr.de

¹ R. Skrotzki, J. Fiedler, T. Herrmannsdörfer, V. Heera, M. Voelskow, A. Mücklich, B. Schmidt, W. Skorupa, G.

Gobsch, M. Helm, and J. Wosnitza Appl. Phys. Lett. **97**, 192505 (2010).

² W. Buckel and R. Hilsch, Z. Phys. **138**, 109 (1954).

³ H. M. Jaeger, D. B. Haviland, B. G. Orr, and A. M. Gold-

- man, Phys. Rev. B **40**, 182 (1989).
- ⁴ J. Fiedler, V. Heera, R. Skrotzki, T. Herrmannsdörfer, M. Voelskow, A. Mücklich, S. Oswald, B. Schmidt, W. Skorupa, G. Gobsch, J. Wosnitza, and M. Helm, Phys. Rev. B **83**, 214504 (2011).
- ⁵ M. Tinkham, *Introduction to Superconductivity* (Dover, NY, 1996).
- ⁶ D. N. Basov and T. Timusk, Rev. Mod. Phys. **77**, 721 (2005).
- ⁷ O. S. Heavens, *Optical properties of thin solid films* (Dover, NY, 1965).
- ⁸ G. V. Kozlov and A. A. Volkov, in *Millimeter and Submillimeter Wave Spectroscopy of Solids*, edited by G. Grüner (Springer, Berlin, 1998), p. 51.
- ⁹ M. Dressel, N. Drichko, B. P. Gorshunov, and A. Pimenov, IEEE J. Sel. Top. Quantum Electron. **14**, 399 (2008) and references therein.
- ¹⁰ A. V. Pronin, A. Pimenov, A. Loidl, A. Tsukada, and M. Naito, Phys. Rev. B **68**, 054511 (2003).
- ¹¹ T. Fischer, A. V. Pronin, J. Wosnitza, K. Iida, F. Kurth, S. Haindl, L. Schultz, B. Holzapfel, and E. Schachinger, Phys. Rev. B **82**, 224507 (2010).
- ¹² R. J. von Gutfeld and A. H. Nethercot, Phys. Rev. Lett. **18**, 855 (1967).
- ¹³ J. P. Carbotte, Rev. Mod. Phys. **62**, 1027 (1990).
- ¹⁴ F. Marsiglio and J. P. Carbotte in *Superconductivity*, edited by K. H. Bennemann and J. B. Ketterson (Springer, Berlin, 2008), vol. 1, p. 73.
- ¹⁵ T. Fischer, PhD Thesis, TU Dresden, 2012.
- ¹⁶ T. T. Chen, J. T. Chen, J. D. Leslie, and H. J. T. Smith, Phys. Rev. Lett. **22**, 526 (1969).
- ¹⁷ R. W. Cohen, B. Abeles, and G. S. Weisbarth, Phys. Rev. Lett. **18**, 336 (1967).
- ¹⁸ H. Wühl, J. E. Jackson, and C. V. Briscoe, Phys. Rev. Lett. **20**, 1496 (1968).
- ¹⁹ G. v. Minnigerode und J. Rothenberg, Z. Phys. **213**, 397 (1968).
- ²⁰ R. E. Harris and D. M. Ginsberg, Phys. Rev. **188**, 737 (1969).